J Intell Robot Syst (2017) 88:449–467
DOI 10.1007/s10846-017-0474-0

Active Fault-Tolerant Control for a Quadrotor with Sensor Faults

Liguo Qin · Xiao He · Rui Yan · Donghua Zhou

Received: 30 August 2016 / Accepted: 5 January 2017 / Published online: 17 January 2017
© Springer Science+Business Media Dordrecht 2017

Abstract An active fault-tolerant control scheme for a quadrotor with velocity sensor faults is presented in this paper. A two-level control scheme is designed to guarantee the quadrotor to track the given trajectory in case of no faults. The control scheme consists of an external-loop Proportion Differentiation (PD) control law and an internal-loop Proportion Integration Differentiation (PID) control law. A fault diagnosis unit is designed to detect and estimate sensor faults. The fault detection is achieved by using a Luenberger observer based residual generator and the fault estimation problem is solved by utilizing a new proposed augment variable observer. A sufficient condition on the existence of the augment variable observer is given based on Linear Matrix Inequalities (LMIs). The uniformly ultimately bounded property of state and fault estimation errors is proved. By combining the external-loop PD control law and the result of fault estimation, a fault-tolerant control law is proposed. Finally, the effectiveness of the scheme is demonstrated by the simulation and experimental results.

Keywords Active fault-tolerant control · Fault diagnosis · Quadrotor · Sensor faults

D. Zhou (✉) · L. Qin · X. He · R. Yan
Department of Automation, TNList, Tsinghua University, Beijing 100084, People's Republic of China
e-mail: zdh@mail.tsinghua.edu.cn

L. Qin
e-mail: qinlg11@mails.tsinghua.edu.cn

X. He
e-mail: hexiao@tsinghua.edu.cn

R. Yan
e-mail: yr15@mails.tsinghua.edu.cn

D. Zhou
College of Electrical Engineering and Automation, Shandong Universityof Science and Technology, Qingdao, People's Republic of China

1 Introduction

In recent years, there has been a surge of interest in the study of unmanned aerial vehicles (UAVs) since UAVs have a wide application in the areas of geological surveying, fire monitoring, rescue mission, etc. Various UAVs such as fixed and rotary wing UAVs have been developed in recent years. Compared with other types of UAVs, quadrotor helicopters have better performance in the aspects such as large payload, great maneuverability and simple manufacture [19].

Recently, researchers have shown an increasing interest in quadrotors. In [4, 6, 17], various mathematical models of a quadrotor such as kinematic and dynamic models were built. Moreover, many control schemes have been proposed which can be used to quadrotors such as Proportion Integration Differentiation (PID) control [9], adaptive control [3, 24], backstepping control [8, 11] and fuzzy control [20]. However, most of the aforementioned literatures have

only considered the case where there is no faults in quadrotros without taking account of faults occurring in quadrotors. In the case that actuator or sensor faults occur, those controllers can not guarantee the normal operation of quadrotors.

In the last decades, researchers have shown an increasing interest in the field of fault diagnosis and fault-tolerant control for quadrotors which play pivot roles in the area of reliability and safety of dynamic systems. The studies on fault diagnosis and fault-tolerant control for quadrotors was reviewed in [27]. It is shown in [27] that these works can be divided into different types according to faults, testbeds, frameworks, problems considered and tools employed. In [5], a robust fault diagnosis problem for a quadrotor with actuator faults was addressed by using an adaptive Thau's observer. The robustness of the fault estimation scheme to magnitude order unbalances, modeling uncertainties, and noise is achieved by solving a presented synthetic robust optimization problem. [16] presented a fault recovery scheme for a quadrotor with actuator faults. The actuator fault was estimated by a parameter estimation algorithm and a nonlinear adaptive controller was developed to guarantee the stability of the closed-loop system based on the fault estimation.

Although some research has been carried out on fault diagnosis and fault-tolerant control for quadrotors with actuator faults, there is a relative paucity of studies considering the case of sensor faults. In some literature such as [18, 23, 25], the fault diagnosis of sensor faults was converted into that of actuator faults. However, the actuator fault diagnosis methods are not feasible for sensor faults in some cases, for instance, when the frequency of the sensor fault is larger than the bandwidth of fault diagnosis observers and when the dynamic system is nonlinear.

Very little research has been carried out on direct fault diagnosis for quadrotors in the presence of sensor faults. In [7], a quadrotor was described as a Lipschitz nonlinear model and a fault diagnosis scheme was designed based on a Thau's observer for the quadrotor with actuator and sensor faults. A fault diagnosis problem for quadrotors with various sensor faults was considered in [1]. A nonlinear identity observer and a generalized observer scheme were used to detect and isolate faults, respectively. In [12], faults in a triaxis accelerometer and a triaxis magnetometer of a quadrotor were detected by the presented two techniques. The first approach was developed based on parameter estimation and the second one was proposed by utilizing set membership estimation theory. Time-varying observers are used to diagnosis sensor faults in quadrotors in some literature. In [10], a robust fault diagnosis scheme was proposed for quadrotors with sensor faults. The quadrotor was modeled as a linear parameter varying system and the fault detection observer is developed based on H_∞ performance. In [15], the fault diagnosis problem for quadrotors with angular accelerator sensor faults was addressed by using a bank of reduced order time-varying observers.

The control performance of quadrotors decreases heavily if there are sensor faults occurring. Fortunately, fault-tolerant control is able to guarantee the flying performance of a quadrotor even if sensor faults occur in the quadrotor. In [2], a fault-tolerant attitude control scheme was designed for quadrotors with sensor faults by using a multi-observer switching strategy. The attitude of the quadrotor was estimated by a bank of nonlinear observers. The results of the observer which has the smallest error were selected to compensate sensor faults. To date, the fault-tolerant control problem for quadrotors with sensor faults has not yet been systematically studied. Moreover, most of the aforementioned works were carried out in a simulation framework, and seldom experimental results on quadrotors with sensor faults have been reported.

In this paper, fault diagnosis and fault-tolerant control problems are investigated for a quadrotor with velocity sensor faults. When there is no fault, a two-level control scheme is developed to guarantee that quadrotors are able to track the given trajectory. The first level is an external-loop Proportion Differentiation (PD) control law while the second one is an internal-loop Proportion Integration Differentiation (PID) control law. Then, a residual generator based on Luenberger observers is designed to detect sensor faults and a novel augment variable observer is proposed to estimate sensor faults. Furthermore, the uniformly ultimately bounded property of estimation errors is proved by using Linear Matrix Inequalities (LMIs). Finally, a fault-tolerant control law is developed by combining the external PD control law and the results of fault estimation.

This paper is an extension of the conference paper [14]. Different from the paper [14], the design of the

parameters of the external-loop PD control law and the internal-loop PID control law is provided in the paper when there is no fault. Moreover, model uncertainties and sensor disturbances are considered during the sensor fault estimation in the paper, which increases the difficulties of fault estimation.

The remaining part of the paper proceeds in the following way. Section 2 presents the fault-tolerant control problem and develops the two-level control scheme. Section 3 proposes the fault diagnosis scheme and the fault-tolerant control law. In Section 4, simulation and experimental results show the effectiveness of the scheme. Finally, conclusions are given in Section 5.

Notation Throughout this paper, $\mathbb{R}$ represents the sets of real numbers. $\mathbb{R}^n$ stands for the sets of real vectors with n dimensions. $\|x\|$ is the Euclidean norm of the vector x. $\|A\|_2$ is the spectral norm of the matrix A. I_n stands for the n by n identity matrix. 0 denotes the zero matrix or zero vector with appropriate dimensions. $W > 0$ represents that the symmetric matrix W is positive definite.

2 Problem Formulation

According to [4] and [26], the following model can be used to describe a quadrotor unmanned helicopter.

$$\begin{cases} m\ddot{p}_x(t) &= (sin\psi sin\phi + cos\psi sin\theta cos\phi)u_z, \\ m\ddot{p}_y(t) &= (-cos\psi sin\phi + sin\psi sin\theta cos\phi)u_z, \\ m\ddot{p}_z(t) &= -mg + (cos\theta cos\phi)u_z, \\ J_x\ddot{\theta}(t) &= u_\theta(t), \\ J_y\ddot{\phi}(t) &= u_\phi(t), \\ J_z\ddot{\psi}(t) &= u_\psi(t), \end{cases} \tag{1}$$

where $p_x \in \mathbb{R}$, $p_y \in \mathbb{R}$ and $p_z \in \mathbb{R}$ are position coordinates along the x axis, y axis and z axis of the earth inertial frame, respectively. $\theta \in \mathbb{R}$, $\phi \in \mathbb{R}$ and $\psi \in \mathbb{R}$ are the pitch, roll and yaw angles of the quadrotor, respectively. m is the mass of the quadrotor and g is the acceleration of gravity. $J_x \in \mathbb{R}$, $J_y \in \mathbb{R}$ and $J_z \in \mathbb{R}$ are the rotation inertial. $u_z \in \mathbb{R}$, $u_\theta \in \mathbb{R}$, $u_\phi \in \mathbb{R}$ and $u_\psi \in \mathbb{R}$ are control inputs of the quadrotor.

Under the assumption that the quadrotor moves in a hovering state and the rotation angles are close to zeros, the quadrotor unmanned helicopter can be described as

$$\begin{cases} \ddot{p}_x(t) &= \theta(t)g, \\ \ddot{p}_y(t) &= -\phi(t)g, \\ \ddot{p}_z(t) &= u_z(t)/m - g, \\ J_x\ddot{\theta}(t) &= u_\theta(t), \\ J_y\ddot{\phi}(t) &= u_\phi(t), \\ J_z\ddot{\psi}(t) &= u_\psi(t). \end{cases} \tag{2}$$

It is noted that the rotation angles of a quadrotor are decoupled in Eq. 2. Therefore, the control schemes and the fault diagnosis schemes can be easily designed along x axis, y axis and z axis, respectively. For simplicity, the fault-tolerant control scheme along x axis is considered in the paper, and the schemes along y and z axes can be derived in a similar manner.

According to the Eq. 2, the dynamic model of the quadrotor along x axis is

$$\begin{cases} \ddot{p}_x(t) &= \theta(t)g, \\ J_x\ddot{\theta}(t) &= u_\theta(t). \end{cases} \tag{3}$$

Define $p_{x_{set}}(t) \in \mathbb{R}$ as the reference trajectory of a quadrotor. Before developing the control scheme, the following assumption is required.

Assumption 1 The given reference trajectory of the quadrotor $p_{x_{set}}(t)$ satisfies that $\forall t \geq 0$, $\dot{p}_{x_{set}}(t)$ and $\ddot{p}_{x_{set}}(t)$ exist, where $\dot{p}_{x_{set}}(t) \in \mathbb{R}$ and $\ddot{p}_{x_{set}}(t) \in \mathbb{R}$ are the first and second derivatives of $p_{x_{set}}(t)$, respectively.

Remark 1 Assumption 1 requires the existence of the first and second derivatives of the reference trajectory. In practice, the trajectory of a quadrotor is limited by its maneuverability. Therefore, it is reasonable to impose restrictions on the reference trajectory of quadrotors.

Figure 1 shows the framework of control scheme when there is no sensor fault. The control scheme consists of two levels. The internal-loop controller is a PID controller which is used to control the rotation angles, and the external-loop controller is a PD controller which is used to control the trajectory of the quadrotor.

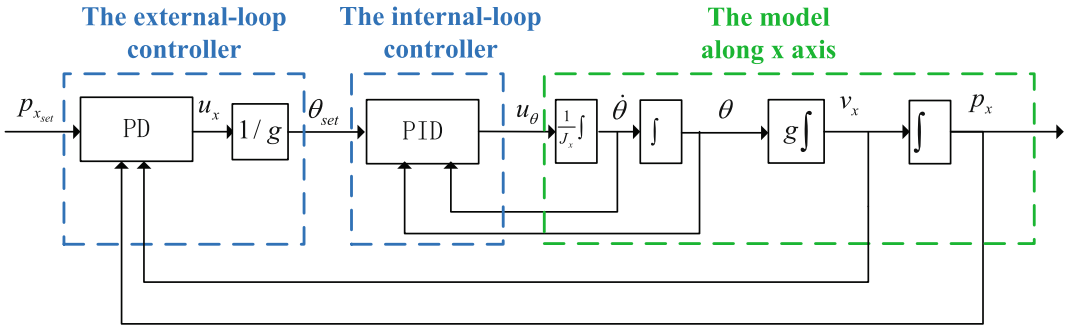

Fig. 1 The framework of control when there are no faults

Under Assumption 1, when there are no sensor faults occurring in quadrotors, the formulation of the external-loop PD controller is as follows.

$$\begin{aligned} u_x(t) &= k_1^p[p_{x_{set}}(t) - p_x(t)] \\ &\quad + k_1^d[\dot{p}_{x_{set}}(t) - v_x(t)] + \ddot{p}_{x_{set}}(t), \end{aligned} \tag{4}$$

where $v_x \in \mathbb{R}$ is the velocity of the quadrotor along x axis. $k_1^p \in \mathbb{R}$ and $k_1^d \in \mathbb{R}$ are controller parameters to be designed.

According to Eq. 4, the tracking signal of the internal-loop controller can be obtained as the following equation.

$$\theta_{set}(t) = u_x(t)/g, \tag{5}$$

where $\theta_{set} \in \mathbb{R}$ is the pitch angle that the quadrotor should track.

Then, the internal-loop PID controller is derived as

$$\begin{aligned} u_\theta(t) &= k_2^p[\theta_{set}(t) - \theta(t)] + k_2^i \int_0^t [\theta_{set}(t) - \theta(t)]dt \\ &\quad + k_2^d \frac{d[\theta_{set}(t) - \theta(t)]}{dt}, \end{aligned} \tag{6}$$

where $k_2^p \in \mathbb{R}$, $k_2^i \in \mathbb{R}$ and $k_2^d \in \mathbb{R}$ are the internal-loop controller parameters to be determined.

Define the position tracking error and angle control error as $e_x = p_{x_{set}} - p_x$ and $e_\theta = \theta_{set} - \theta$, respectively. The following two propositions provide the design of the parameters of the external-loop and internal-loop controllers.

Proposition 1 *Given the model* (3) *and the external-loop PD controller* (4)*, the position tracking error, e_x, reaches to zero asymptotically if $k_1^p > 0$ and $k_1^d > 0$.*

Proof Since $e_x(t) = p_{x_{set}}(t) - p_x(t)$, it follows that

$$\begin{aligned} \dot{e}_x(t) &= \dot{p}_{x_{set}}(t) - v_x(t), \\ \ddot{e}_x(t) &= \ddot{p}_{x_{set}}(t) - u_x(t) = -k_1^p e_x(t) - k_1^d \dot{e}_x(t). \end{aligned} \tag{7}$$

Then it can be gained that

$$\begin{bmatrix} \dot{e}_x(t) \\ \ddot{e}_x(t) \end{bmatrix} = \begin{bmatrix} 0 & 1 \\ -k_1^p & -k_1^d \end{bmatrix} \begin{bmatrix} e_x(t) \\ \dot{e}_x(t) \end{bmatrix}. \tag{8}$$

The characteristic equation of the Eq. 8 is as

$$s^2 + k_1^d s + k_1^p = 0. \tag{9}$$

Since $k_1^p > 0$ and $k_1^d > 0$, the real parts of the roots of the Eq. 9 are both negative, which means that the Eq. 8 is stable and $e_x(t)$ reaches to zero asymptotically.

This ends the proof. □

Proposition 2 *Given the model* (3) *and the internal-loop PID controller* (6)*, the angle control error, e_θ, reaches to zero asymptotically if $\dddot{\theta}_{set}(t) = 0$, $k_2^p > 0$, $k_2^d > 0$, $k_2^i > 0$ and $k_2^p k_2^d > k_2^i J_x$.*

Proof Since $\dddot{\theta}_{set}(t) = 0$ and $e_\theta(t) = \theta_{set}(t) - \theta(t)$, it follows that

$$\begin{aligned} \dot{e}_\theta(t) &= \dot{\theta}_{set}(t) - \dot{\theta}(t), \\ \ddot{e}_\theta(t) &= \ddot{\theta}_{set}(t) - \ddot{\theta}(t), \\ \dddot{e}_\theta(t) &= \dddot{\theta}_{set}(t) - \dddot{\theta}(t) = \dddot{\theta}_{set}(t) - \frac{\dot{u}_\theta(t)}{J_x} \\ &= -\frac{k_2^d \ddot{e}_\theta(t)}{J_x} - \frac{k_2^p \dot{e}_\theta(t)}{J_x} - \frac{k_2^i e_\theta(t)}{J_x}. \end{aligned} \tag{10}$$

Then it can be gained that

$$\begin{bmatrix} \dot{e}_\theta(t) \\ \ddot{e}_\theta(t) \\ \dddot{e}_\theta(t) \end{bmatrix} = \begin{bmatrix} 0 & 1 & 0 \\ 0 & 0 & 1 \\ -\frac{k_2^i}{J_x} & -\frac{k_2^p}{J_x} & -\frac{k_2^d}{J_x} \end{bmatrix} \begin{bmatrix} e_\theta(t) \\ \dot{e}_\theta(t) \\ \ddot{e}_\theta(t) \end{bmatrix}. \tag{11}$$

The characteristic equation of the system (11) is as follows.

$$s^3 + \frac{k_2^d}{J_x}s^2 + \frac{k_2^p}{J_x}s + \frac{k_2^i}{J_x} = 0. \tag{12}$$

According to the Roth-Hurwitz stability criterion, if $k_2^p > 0$, $k_2^d > 0$, $k_2^i > 0$ and $k_2^p k_2^d > k_2^i J_x$, the real parts of the roots of Eq. 12 are all less than zeros, which means that the system (11) is stable and $e_\theta(t)$ reaches to zero asymptotically.

This completes the proof. □

Remark 2 Since we assume that the quadrotor moves in a hovering state and the rotation angles are close to zeros, it is reasonable to assume that $\dddot{\theta}_{set}(t) = 0$ in Proposition 2. In practice, the parameters of the external-loop controller and the internal-loop controller should be determined according to the conditions in Propositions 1 and 2 as well as the real situation of quadrotors since there are nonlinear dynamics, noise and uncertainties disturbing the flying of quadrotors.

In practice, the response time of the internal-loop controller is much smaller than that of the external-loop controller which means that the control of the rotation angles is faster than that of the displacement. Therefore, the response time of the control of rotation angles can be neglected and the model from θ_{set} to θ in Fig. 1 can be seen as a proportion. It follows that the model from u_x to p_x can be considered as a second-order integrator. By taking model uncertainties and sensor disturbances into account, the model of a quadrotor is derived as the following equation.

$$\begin{cases} \dot{p}_x(t) &= v_x(t), \\ \dot{v}_x(t) &= u_x(t) + d(t), \\ y_1(t) &= p_x(t) + w_1(t), \\ y_2(t) &= v_x(t) + f_s(t) + w_2(t), \end{cases} \tag{13}$$

where $y_1 \in \mathbb{R}$ and $y_2 \in \mathbb{R}$ are the outputs of displacement and velocity sensors, respectively. $f_s \in \mathbb{R}$ is the velocity sensor fault. $d \in \mathbb{R}$ represents the model uncertainty or the actuator fault. $w_1 \in \mathbb{R}$ and $w_2 \in \mathbb{R}$ are sensor disturbances.

The state space model of the quadrotor is as follows.

$$\begin{cases} \dot{x}(t) = Ax(t) + Bu(t) + Ef(t), \\ y(t) = Cx(t) + \Gamma f(t) + w(t), \end{cases} \tag{14}$$

where $x = [p_x v_x]^T$, $u = u_x$, $y = [y_1 y_2]^T$, $f = [d f_s]^T$, $w = [w_1 w_2]^T$. The values of parameters in Eq. 14 are as follows.

$$A = \begin{bmatrix} 0 & 1 \\ 0 & 0 \end{bmatrix}, B = \begin{bmatrix} 0 \\ 1 \end{bmatrix}, C = \begin{bmatrix} 1 & 0 \\ 0 & 1 \end{bmatrix},$$
$$E = \begin{bmatrix} 0 & 0 \\ 1 & 0 \end{bmatrix}, \Gamma = \begin{bmatrix} 0 & 0 \\ 0 & 1 \end{bmatrix}.$$

The objective of the paper is to find an active fault-tolerant control law like the following equation such that the quadrotor is able to track the given trajectory no matter whether there are sensor faults or not.

$$u_x(t) = \begin{cases} u_x^n(t) & \text{in fault free case,} \\ u_x^f(t) & \text{in fault case.} \end{cases} \tag{15}$$

Before designing the fault-tolerant control law, some assumptions are required.

Assumption 2 The norm of the uncertainty and sensor disturbances satisfy $\|\dot{d}(t)\| \leq \rho$, $\|\dot{w}_2(t)\| \leq \delta_1$, and $\|w(t)\| \leq \delta_2$, where ρ, δ_1 and δ_2 are known positive real numbers.

Assumption 3 The formulation of the sensor fault $f_s(t)$ is assumed to be $f_s(t) = \gamma(t - T)\xi(t)$, where T is the time instant when the fault occurs and $\gamma(t - T)$ is the sensor fault profile whose formulation is as

$$\gamma(t - T) = \begin{cases} 0 & t < T, \\ 1 & t \geq T. \end{cases} \tag{16}$$

$\xi(t)$ is the signal representing the amplitude of the velocity sensor fault.

Remark 3 In Eq. 13, the model from u_x to p_x in Fig. 1 is regarded as a second-order integrator. Such processing still results in model uncertainties even if the rotation angles of the quadrotor are small. Therefore, $d(t)$ is introduced to represent the model uncertainties. Moreover, $d(t)$ can also be used to denote actuator faults of a quadrotor as described in literature [21, 22].

Remark 4 The velocity used in the paper is gained by fusing data from the Global Positioning System (GPS) and the Inertial Navigation System (INS) of the quadrotor. As shown in Fig. 2, the velocity fault in the paper is described as an offset of the velocity. It is noted that such kind of description is able to represent faults in GPS or INS.

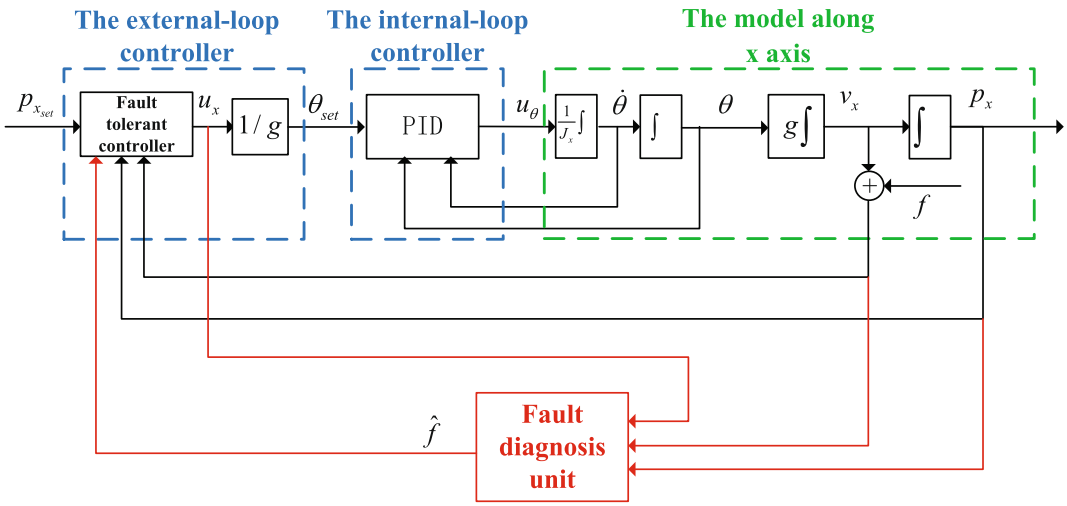

Fig. 2 The framework of the fault-tolerant control

Remark 5 Since only velocity sensor faults are considered and there is no direct feedback from the velocity sensor to the internal-loop controller, sensor faults cannot directly disturb the control of the attitudes of quadrotors. The effect of velocity sensor faults can be neutralized by the fault-tolerant control law of the external-loop controller. Hence, in the paper, we only consider the design of the fault-tolerant control law for the external-loop controller.

Remark 6 The amplitude of the sensor fault signal considered in the paper cannot be arbitrarily large because the linear model (2) of the quadrotor is reasonable only if the rotation angles of the quadrotor are small. Moreover, in the experiments in Section 4.2, the range of rotation angles measured in radians is $[-\frac{\pi}{18}, \frac{\pi}{18}]$.

3 Design of Fault-Tolerant Control

This section presents the design of the fault-tolerant control law for quadrotors with sensor faults. Figure 2 illustrates the framework of the fault-tolerant control scheme. In the scheme, a fault diagnosis unit is developed to detect and estimate the velocity sensor fault by using the input and output information of the quadrotor. A new control law is designed to tolerate the velocity sensor fault by combining the fault estimation and the control law in fault free case.

3.1 Fault Detection

The fault detection of the quadrotor is achieved by a residual generator developed based on a Lunenberger observer. The formulation of the generator is as

$$\begin{cases} \dot{\hat{x}}_r(t) = A\hat{x}_r(t) + Bu(t) + L[y(t) - C\hat{x}_r(t)], \\ r(t) = \quad y(t) - C\hat{x}_r(t), \end{cases} \tag{17}$$

where $\hat{x}_r \in \mathbb{R}^2$ is the state estimation of the quadrotor. $r \in \mathbb{R}^2$ is the residual vector of the generator. L is the parameter to be designed. Since the pair (A, C) is observable, it is obvious that there exists a matrix L such that the matrix $A - LC$ is stable.

Define $J_{det} \in \mathbb{R}$ as the residual evaluation function and the formulation of J_{det} is

$$J_{det}(t) = \|r(t)\|. \tag{18}$$

The fault detection scheme is

$$\begin{cases} J_{det}(t) \le J_{th} \Rightarrow \text{normal}, \\ J_{det}(t) > J_{th} \Rightarrow \text{a fault occurs}, \end{cases} \tag{19}$$

where $J_{th} \in \mathbb{R}$ is the threshold of the fault detection scheme and the value of J_{th} can be designed in experiments according to the experience of experts, disturbances and uncertainties of a quadrotor.

Remark 7 Since the model of a quadrotor is decoupled along x, y, and z axes, velocity sensor faults along

different axes are also decoupled. The fault isolation of different velocity sensor faults along different axes can be achieved by the fault detection along each axis. In a more complex case where the sensor faults are not decoupled, the fault isolation can be achieved by fault matching estimators. The detailed algorithm can be found in the literature [13], and is omitted here for simplicity.

3.2 Fault Estimation

The fault estimation is achieved by an augment variable observer. The formulation of the observer is as follows.

$$\begin{cases} \dot{\hat{x}}(t) = A\hat{x}(t) + Bu(t) + E\hat{f}(t) \\ \qquad\quad +G[y(t) - C\hat{x}(t) - \Gamma\hat{f}(t)], \\ \dot{v}(t) = M_1[CA\hat{x}(t) + CBu(t) + CE\hat{f}(t)] \\ \qquad\quad +M_2[y(t) - C\hat{x}(t) - \Gamma\hat{f}(t)], \\ \hat{f}(t) = v(t) - M_1 y(t), \end{cases} \tag{20}$$

where $\hat{x} \in \mathbb{R}^2$ is the state estimation of the quadrotor. $v \in \mathbb{R}^2$ is the augment variable. $\hat{f} \in \mathbb{R}^2$ is the estimation of the uncertainty and the sensor fault. G and M_2 are parameters to be determined. M_1 satisfies

$$M_1\Gamma = -\begin{bmatrix} 0 & 0 \\ 0 & 1 \end{bmatrix}. \tag{21}$$

Therefore, we can design $M_1 = -\Gamma$.

Define the state estimation error and the fault estimation error as the following equations.

$$\begin{aligned} e(t) &= x(t) - \hat{x}(t), \\ \eta(t) &= f(t) - \hat{f}(t). \end{aligned} \tag{22}$$

Define the error vector $\zeta = [e^T \quad \eta^T]^T$. Define matrices $\bar{A}, \bar{C}, \bar{G}, D_1, D_2$ as follows:

$$\begin{aligned} &\bar{A} = \begin{bmatrix} A & E \\ M_1CA & M_1CE \end{bmatrix}, \bar{C} = \begin{bmatrix} C & \Gamma \end{bmatrix}, \bar{G} = \begin{bmatrix} G \\ M_2 \end{bmatrix}, \\ &D_1 = \begin{bmatrix} 0 & 0 & 1 & 0 \end{bmatrix}^T, D_2 = \begin{bmatrix} 0 & 0 & 0 & 1 \end{bmatrix}^T. \end{aligned} \tag{23}$$

The following theorem presents a sufficient condition on the existence of the augment observer and the algorithm to design the parameters.

Theorem 1 *Given scalars $\varepsilon_1 > 0$, $\varepsilon_2 > 0$, $\varepsilon_3 > 0$ and a symmetric positive definite matrix $Q > 0$, if there exist a matrix K and a symmetric positive definite matrix $P > 0$ such that the following condition holds*

$$\begin{bmatrix} P\bar{A} + \bar{A}^T P - K\bar{C} - \bar{C}^T K + Q & PD_1 & PD_2 & K \\ D_1^T P & -\frac{1}{\varepsilon_1} & 0 & 0 \\ D_2^T P & 0 & -\frac{1}{\varepsilon_2} & 0 \\ K^T & 0 & 0 & -\frac{I_2}{\varepsilon_3} \end{bmatrix} < 0, \tag{24}$$

then the fault estimation scheme (20) is able to realize that e and η are uniformly ultimately bounded. Moreover, the boundaries of e and η satisfy

$$\lim_{t\to\infty} \|\zeta\| \le \frac{\beta}{\lambda_{min}\{P\}\alpha}, \tag{25}$$

where $\alpha = \frac{\lambda_{min}\{Q\}}{\lambda_{max}\{P\}}$, $\beta = \frac{\rho}{\varepsilon_1} + \frac{\delta_1}{\varepsilon_2} + \frac{\delta_2}{\varepsilon_3}$. $\lambda_{min}\{P\}$ and $\lambda_{min}\{Q\}$ are the minimum eigenvalues of the matrix P and Q, respectively. $\lambda_{max}\{P\}$ is the maximum eigenvalue of the matrix P. Furthermore, the parameters $\bar{G}$ can be designed as $\bar{G} = P^{-1}K$.

Proof According to Eqs. 14 and 20, it can be gained that

$$\begin{aligned} \dot{e}(t) &= \dot{x} - \dot{\hat{x}}(t) \\ &= (A - GC)e(t) + (E - G\Gamma)\eta(t) - Gw(t), \\ \dot{\eta}(t) &= \dot{f}(t) - \dot{\hat{f}}(t) = \dot{f}(t) - \dot{v}(t) + M_1\dot{y}(t) \\ &= M_1[CAx(t) + CBu(t) + CEf(t) + \dot{w}(t)] \\ &\quad -\dot{v}(t) + [10]^T\dot{d}(t) \\ &= (M_1CA - M_2C)e(t) + (M_1CE - M_2\Gamma)\eta(t) \\ &\quad -[01]^T\dot{w}_2(t) - M_2w(t) + [10]^T\dot{d}(t). \end{aligned}$$

It follows that

$$\begin{bmatrix} \dot{e}(t) \\ \dot{\eta}(t) \end{bmatrix} = \begin{bmatrix} A - GC & E - G\Gamma \\ M_1CA - M_2C & M_1CE - M_2\Gamma \end{bmatrix} \begin{bmatrix} e(t) \\ \eta(t) \end{bmatrix} + D_1\dot{d}(t) - D_2\dot{w}_2(t) - \bar{G}w(t). \tag{26}$$

Then we can gain

$$\dot{\zeta} = (\bar{A} - \bar{G}\bar{C})\zeta + D_1\dot{d}(t) - D_2\dot{w}_2(t) - \bar{G}w(t). \tag{27}$$

Given a symmetric positive matrix $P > 0$, define a function $V(t) = \zeta^T(t)P\zeta(t)$. It can be gained that

$$\begin{aligned}\dot{V}(t) &= \zeta^T(t)[P(\bar{A}-\bar{G}\bar{C})+(\bar{A}-\bar{G}\bar{C})^T P]\zeta(t)\\ &\quad +2\zeta^T(t)PD_1\dot{d}(t)-2\zeta^T(t)PD_2\dot{w}(t)\\ &\quad -2\zeta^T(t)P\bar{G}w(t)\\ &\le \zeta^T(t)[P(\bar{A}-\bar{G}\bar{C})+(\bar{A}-\bar{G}\bar{C})^T P]\zeta(t)\\ &\quad +\varepsilon_1\zeta^T(t)PD_1D_1^T P\zeta(t)+\frac{\rho_1}{\varepsilon_1}\\ &\quad +\varepsilon_2\zeta^T(t)PD_2D_2^T P\zeta(t)+\frac{\delta_1}{\varepsilon_2}\\ &\quad +\varepsilon_3\zeta^T(t)P\bar{G}\bar{G}^T P\zeta(t)+\frac{\delta_2}{\varepsilon_3}.\end{aligned} \tag{28}$$

According to Eq. 24 and Schur Complementary Lemma, we can gain that

$$\begin{aligned}P(\bar{A}-\bar{G}\bar{C})+(\bar{A}-\bar{G}\bar{C})^T P+\varepsilon_1 PD_1D_1^T P\\ +\varepsilon_2 PD_2D_2^T P+\varepsilon_3 P\bar{G}\bar{G}^T P\le -Q.\end{aligned} \tag{29}$$

Then, it is obvious that

$$\begin{aligned}\dot{V}(t) &\le -\zeta^T(t)Q\zeta(t)+\frac{\rho}{\varepsilon_1}+\frac{\delta_1}{\varepsilon_2}+\frac{\delta_2}{\varepsilon_3}\\ &\le -\alpha V(t)+\beta,\end{aligned} \tag{30}$$

According to Eq. 30, it follows that

$$\lim_{t\to\infty} V(t) \le \frac{\beta}{\alpha}. \tag{31}$$

Moreover, we can get

$$\lim_{t\to\infty} \|\zeta(t)\| \le \frac{\beta}{\lambda_{min}\{P\}\alpha}. \tag{32}$$

Therefore, $e(t)$ and $\eta(t)$ are uniformly ultimately bounded. This ends the proof. □

Corollary 1 *If $\rho = \delta_1 = \delta_2 = 0$, the fault estimation scheme (20) can estimate states, sensor faults and uncertainties asymptotically, i.e., $\lim_{t\to\infty} e(t) = 0$ and $\lim_{t\to\infty}\eta(t) = 0$.*

Proof If $\rho = \delta_1 = \delta_2 = 0$, according to Eq. 27, it follows that

$$\dot{\zeta} = (\bar{A}-\bar{G}\bar{C})\zeta. \tag{33}$$

According to Eq. 23, we can gain that the pair $(\bar{A}, \bar{C})$ is observable. Therefore, there exist a matrix $\bar{G}$ such that the matrix $\bar{A}-\bar{G}\bar{C}$ is stable. It is easy to gain that

$$\lim_{t\to\infty}\zeta(t) = 0.$$

This ends the proof. □

Remark 8 In some literature such as [18, 23, 25], sensor faults are estimated by means of changing the sensor faults into actuator faults through linear transformation. However, the weakness of the idea is that the high-frequency information in the sensor fault signals will be filtered since the linear transformation is a kind of low-pass filter processing. The presented fault estimation scheme is able to reconstruct time-varying high-frequency sensor fault signals through direct estimation for the sensor faults by introducing an augment variable.

Remark 9 In fact, the fault estimation scheme (20) not only is applicable to 2-dimension systems but also can be extended to a general linear system. Results in Theorem 1 and Corollary 1 are also feasible to general linear systems.

3.3 Fault-Tolerant Control

When there is no sensor fault, the fault-tolerant control law can be designed as follows.

$$\begin{aligned}u_x^n(t) &= k_1^p[p_{x_{set}}(t)-y_1(t)]+k_1^d[\dot{p}_{x_{set}}(t)-y_2(t)]\\ &\quad +\ddot{p}_{x_{set}}(t).\end{aligned} \tag{34}$$

When the sensor fault is detected, the fault-tolerant control law is changed into the following equation.

$$\begin{aligned}u_x^f(t) &= k_1^p[p_{x_{set}}(t)-y_1(t)]\\ &\quad +k_1^d[\dot{p}_{x_{set}}(t)-y_2(t)+\hat{f}_s(t)]+\ddot{p}_{x_{set}}(t).\end{aligned} \tag{35}$$

Remark 10 If the amplitude of the sensor fault signal is small, the sensor fault cannot be detected by the fault detect scheme presented in the paper. In this case, the control law (34) can still guarantee the stability of the quadrotor though the tracking error of the quadrotor is not able to converge to zero asymptotically.

4 Simulation and Experimental Result

In this section, simulations and experiments are carried out to demonstrate the effectiveness of the presented active fault-tolerant control scheme.

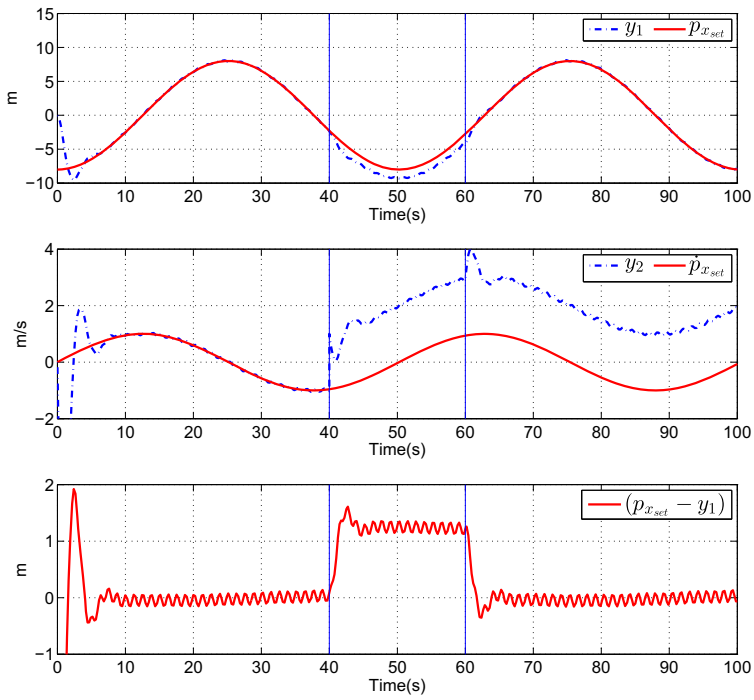

Fig. 3 Sensor outputs in case 1 of the simulation

4.1 Simulation

In the simulation, the dynamic of a quadrotor along x axis described as Eq. 13 is considered. The fault detection, fault estimation and fault-tolerant schemes are designed according to Eqs. 17, 20 and 15, respectively.

The given trajectory of the quadrotor along x axis is $p_{x_{set}}(t) = 8sin(\frac{1}{8}t - \frac{\pi}{2})$. The values of parameters of control law are $k_1^p = 2$, $k_1^d = 1.2$. The model uncertainty is $d(t) = 0.1sin(0.1t)$. The sensor disturbances are $w_1(t) = 0.1sin(5t - \frac{\pi}{2})$, $w_2(t) = 0.05sin(5t)$. The boundary of the uncertainty and disturbances are $\rho = 0.01$, $\delta_1 = 0.25$, $\delta_2 = 0.12$.

The fault detection threshold is $J_{th} = 0.2$. Let $\varepsilon_1 = \varepsilon_2 = \varepsilon_3 = 0.1$. Let $Q = 0.1 \times I_4$. The parameters

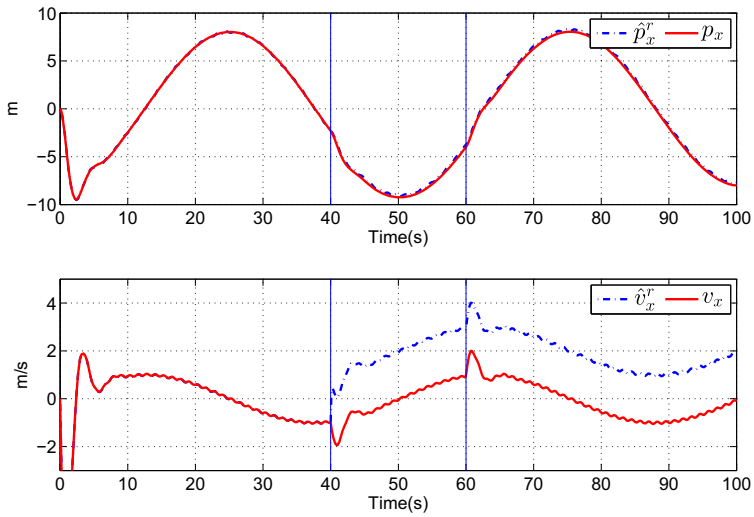

Fig. 4 State estimation in the residual generator in case 1 of the simulation

of fault detection scheme and fault estimation scheme are as follows.

$$
\begin{aligned}
L &= \begin{bmatrix} 10 & 1 \\ 0 & 11 \end{bmatrix}, E = \begin{bmatrix} 0 & 0 \\ 1 & 0 \end{bmatrix}, \Gamma = \begin{bmatrix} 0 & 0 \\ 0 & 1 \end{bmatrix}, \\
M_1 &= -\begin{bmatrix} 0 & 0 \\ 0 & 1 \end{bmatrix}, \\
P &= \begin{bmatrix} 14.9544 & -14.7069 & 7.0455 & -0.1323 \\ -14.7069 & 27.2297 & -15.2675 & 5.8591 \\ 7.0455 & -15.2675 & 15.6383 & -0.5515 \\ -0.1323 & 5.8591 & -0.5515 & 5.4304 \end{bmatrix}, \\
K &= \begin{bmatrix} 9.4406 & 0.0326 \\ -0.0058 & 9.4267 \\ 0.0071 & 0.0073 \\ 0.0042 & 9.4365 \end{bmatrix}, \\
G &= \begin{bmatrix} 3.2726 & -0.0001 \\ 3.6645 & 0.0217 \end{bmatrix}, \\
M_2 &= \begin{bmatrix} 1.9742 & 0.0824 \\ -3.6729 & 1.7227 \end{bmatrix}. \qquad (36)
\end{aligned}
$$

We considered two kinds of sensor faults. In case 1, a constant sensor fault is considered and the formulation of the fault is

$$
f_s(t) = \begin{cases} 0m/s & t < 40s, \\ 2m/s & t \geq 40s. \end{cases} \qquad (37)
$$

In case 2, a sine function sensor fault is taken into account. The formulation of the sine sensor fault is

$$
f_s(t) = \begin{cases} 0m/s & t < 50s, \\ 2.5sin[0.5(t-50)]m/s & t \geq 50s. \end{cases} \qquad (38)
$$

In each case, the simulation time is $100s$. To show the impact of the sensor fault on the normal control law, the time instant when we adopt the fault-tolerant control law is $20s$ later than the time instant when the fault is detected. In the following figures, the first blue vertical line stands for the time instant when the sensor fault occurs, and the second blue vertical line denotes the time instant at which the fault-tolerant control law is adopted.

Figure 3 shows the output of sensors in the first case of the simulation. In the first subgraph of Fig. 3, the red solid line shows the given reference trajectory and the blue dash dot line illustrates the position sensor output. In the second subgraph, the red solid line illustrates the given velocity and the blue dash dot line demonstrates the velocity sensor output. The third subgraph shows the tracking error along x axis. It can be seen that the fault can be tolerated after the fault-tolerant control law is adopted.

Figure 4 illustrates the state estimation of the observer in the fault detection residual generator in case 1 of the simulation. Figure 5 shows the values of residuals and residual evaluation function in case 1 of the simulation. From the second subgraph of the Fig. 5, it can be seen that the sensor fault can be detected after it occurs.

Figure 6 demonstrates the state estimation of fault estimator in case 1 of the simulation. The state and fault cannot be estimated accurately since the uncertainty and disturbances. However, the state estimate errors and fault estimate errors are obviously bounded.

Figures 7, 8, 9, 10 show the similiar results in case 2 of the simulation.

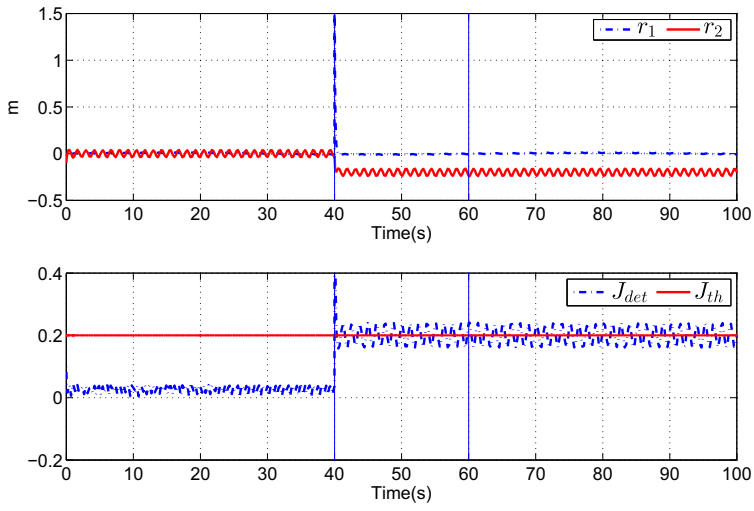

Fig. 5 Residuals and the residual evaluation function in case 1 of the simulation

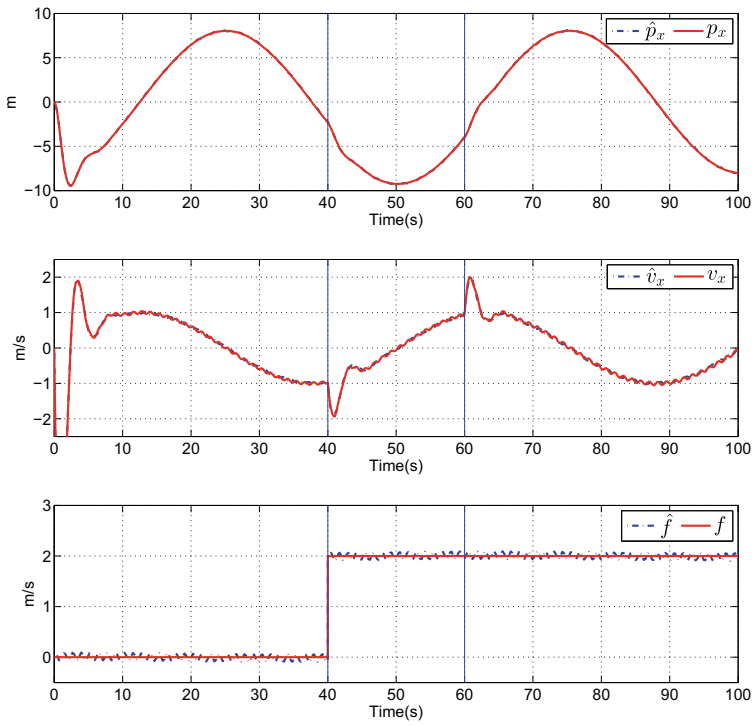

Fig. 6 States and fault estimation in the fault estimator in case 1 of the simulation

4.2 Experimental Results

In the section, an experiment is carried out to demonstrate the effectiveness of the presented fault-tolerant control law by using a real quadrotor which is shown in Fig. 11.

In the experiment, the quadrotor flys along a circle in the $x - O - y$ plane and the position coordinate

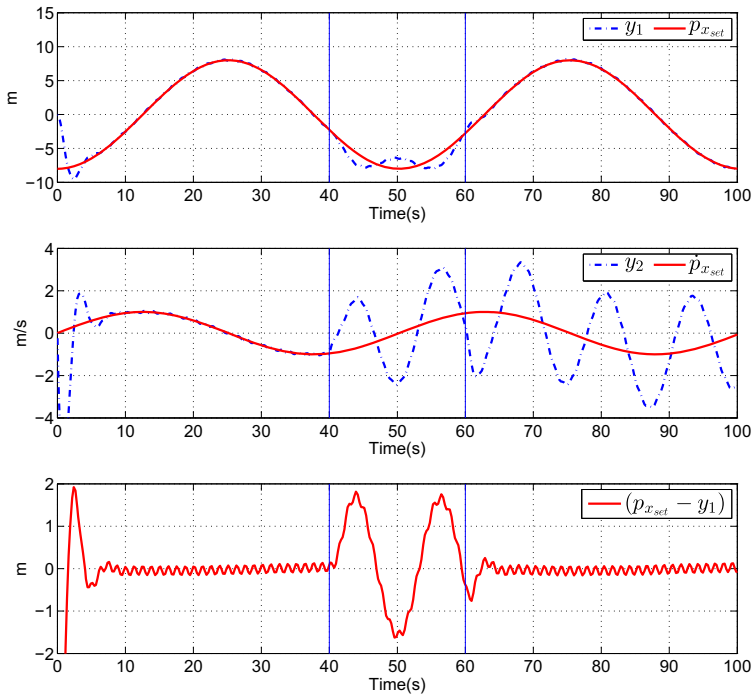

Fig. 7 Sensor outputs in case 2 of the simulation

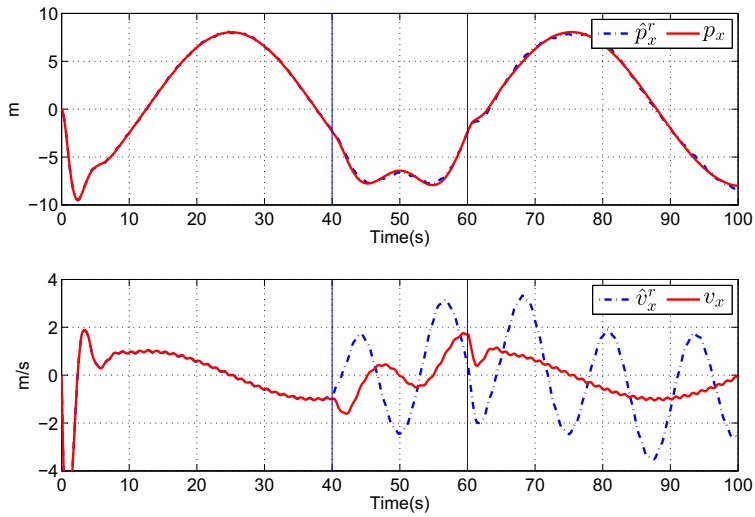

Fig. 8 State estimation in the residual generator in case 2 of the simulation

along z axis is a constant. The given trajectory and the given velocity of the quadrotor in the $x-O-y$ plane is as follows.

$$p_{x_{set}} = 6sin(\tfrac{1}{6}t - \tfrac{\pi}{2})(m),\ \dot{p}_{x_{set}} = sin(\tfrac{1}{6}t)(m/s),$$
$$p_{y_{set}} = 6sin(\tfrac{1}{6}t)(m),\ \dot{p}_{y_{set}} = sin(\tfrac{1}{6}t + \tfrac{\pi}{2})(m/s).$$

The parameters in the external-loop controller are $k_1^p = 3, k_1^d = 3$. Let $\varepsilon_1 = 10, \varepsilon_2 = 1, \varepsilon_3 = 0.001$. Let $Q = 0.1 \times I_4$. The value of parameters in Eq. 17 and Eq. 20 are as follows.

$$L = \begin{bmatrix} 1 & 1 \\ 0 & 2 \end{bmatrix}, E = \begin{bmatrix} 0 & 0 \\ 1 & 0 \end{bmatrix}, \Gamma = \begin{bmatrix} 0 & 0 \\ 0 & 1 \end{bmatrix},$$
$$M_1 = -\begin{bmatrix} 0 & 0 \\ 0 & 1 \end{bmatrix},$$
$$P = \begin{bmatrix} 309.2073 & -54.6997 & 4.9237 & -0.4887 \\ -54.6997 & 32.6595 & -1.9012 & 17.8380 \\ 4.9237 & -1.9012 & 0.3501 & -0.0157 \\ -0.4887 & 17.8380 & -0.0157 & 17.7194 \end{bmatrix},$$
$$K = \begin{bmatrix} 998.5008 & -2.4853 \\ 0.7489 & 1001.2238 \\ -0.06389 & -0.1107 \\ 0.2237 & 1000.3135 \end{bmatrix},$$
$$G = \begin{bmatrix} 14.0269 & 0.0616 \\ 85.4555 & 0.0206 \end{bmatrix},$$
$$M_2 = \begin{bmatrix} 262.8002 & 1.4575 \\ -85.3953 & 56.4353 \end{bmatrix}. \quad (39)$$

We also consider two kinds of sensor faults in the experiment. In case 1, the experiment time is 397s.

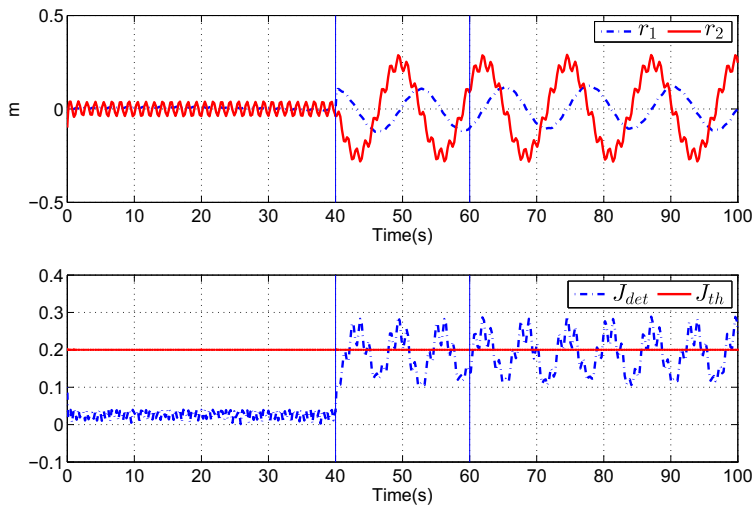

Fig. 9 Residuals and the residual evaluation function in case 2 of the simulation

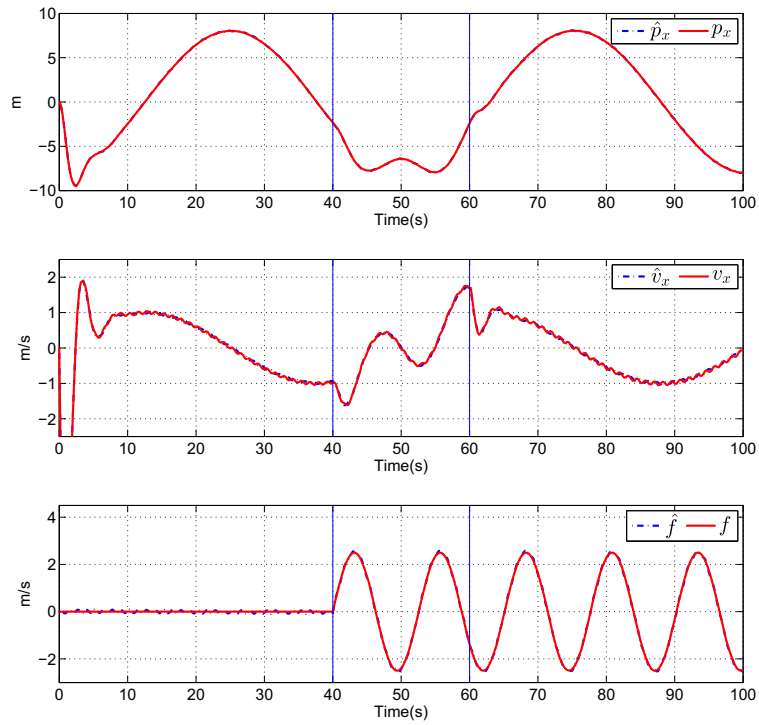

Fig. 10 States and fault estimation in the fault estimator in case 2 of the simulation

The sensor fault is a constant offset and occurs at 322.8975s. The formulation of the sensor fault in case 1 is as

$$f(t) = \begin{cases} 0m/s & t < 322.8975s, \\ 2m/s & t \geq 322.8975s. \end{cases}$$

To show the impact of the velocity sensor fault, we adopt the fault-tolerant control several seconds later than the fault detect time instant. In all the following figures, the first blue vertical line illustrates the time instant when the sensor fault occurs, and the second blue vertical line demonstrates the time instant when the fault-tolerant control law is adopted.

The given trajectory and sensor outputs of the quadrotor are shown in Fig. 12. In the first subgraph of Fig. 12, the given trajectory of the quadrotor is represented by the red solid line, and the position sensor output is illustrated by the blue dash dot line. Looking at the Fig. 12, it is apparent that after the sensor fault occurs, the trajectory of the quadrotor deviates from the given trajectory. After the fault-tolerant control law is adopted at 357.8975s, the trajectory return back to the given trajectory. The second subgraph of Fig. 12 displays the velocity sensor output and the given velocity. The tracking error of the quadrotor is presented in the third subgraph of Fig. 12.

The results of the position estimation and velocity estimation of the residual generator in the first case of the experiment are illustrated in Fig. 13. It can be seen that the state estimations cannot track true value of the state after sensor fault occurs. Figure 14 provides the values of the residual and the residual evaluation

Fig. 11 The picture of a quadrotor unmanned helicopter

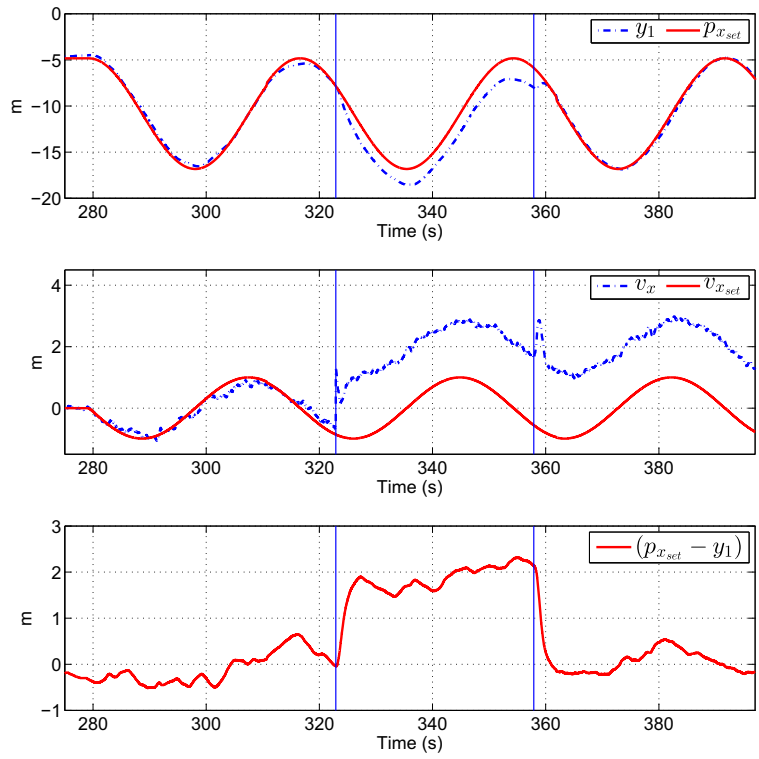

Fig. 12 Outputs of sensors in case 1 of the experiment

function. The fault detection threshold is $J_{th} = 1.5$. It is obvious that after the fault occurs, J_{det} is larger than J_{th}, which means that the fault detection is achieved.

Figure 15 displays the results of state estimation and fault estimation in the augment variable observer. As can be seen from the first and second subgraphs of Fig. 15, the values of state estimation are close to that of the states. The fault estimation results are shown in the third subgraph of Fig. 15. Since there are disturbances and model uncertainties in the experiment, the error of fault estimation cannot accurately converge to zero. The video of the experiment in case 1 of the experiment can be found at https://youtu.be/c4R3ovWWdCk.

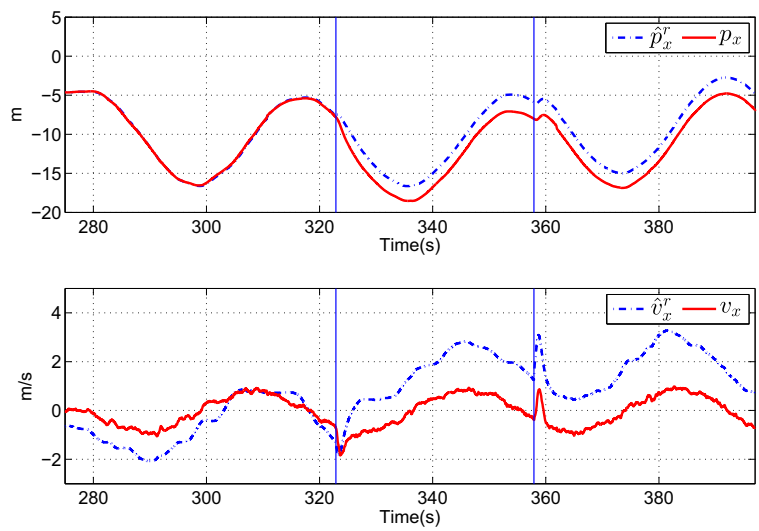

Fig. 13 State estimation in the residual generator in case 1 of the experiment

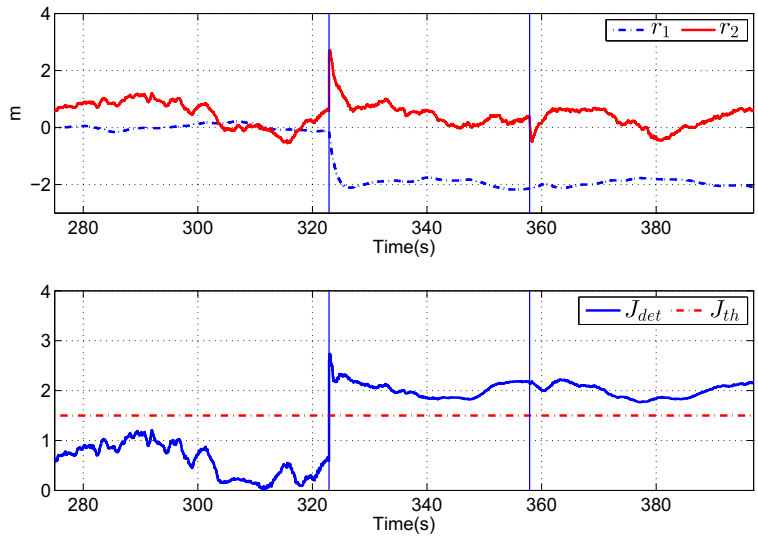

Fig. 14 Residuals and the residual evaluation function in case 1 of the experiment

In case 2, the total experimental time is 260s. The sensor fault is a sine function and occurs at 184.3350s. The formulation of the sensor fault in this case is as

$$f(t) = \begin{cases} 0m/s & t < 184.3350s, \\ 2sin[0.2\pi(t - 184.3350)]m/s & t \geq 184.3350s. \end{cases}$$

The sensor outputs of the quadrotor are shown in Fig. 16. It is apparent from the figure that the quadrotor is not able to track the given trajectory under the normal control law when the sensor fault occurs, and the fault is tolerated after the fault-tolerant control law is adopted at 221.3400s. The tracking error of the quadrotor is illustrated in the third subgraph of Fig. 16.

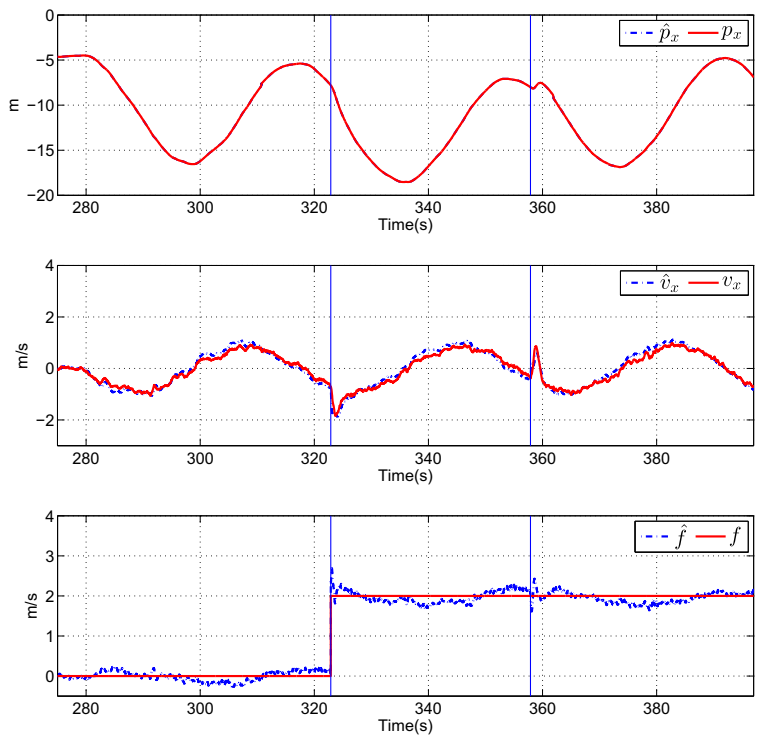

Fig. 15 States and fault estimation in the fault estimator in case 1 of the experiment

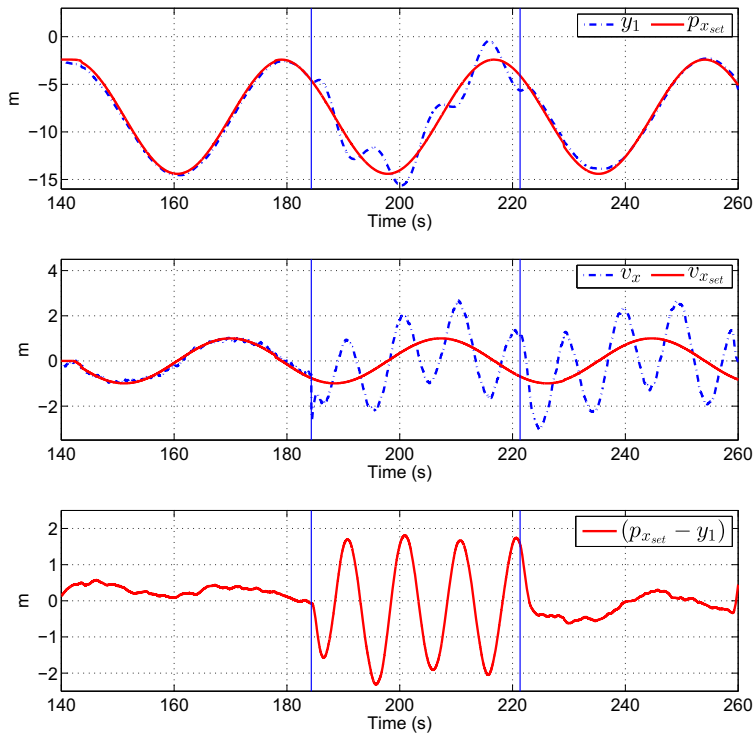

Fig. 16 Outputs of sensors in case 2 of the experiment

The results of state estimation of residual generator and fault detection are displayed in Figs. 17 and 18, respectively. As shown in the second subgraph of Fig. 18, the velocity sensor fault can be detected after the sensor fault occurs.

Figure 19 presents the results of state and fault estimation. The video of the experiment in case 2 can be found at https://youtu.be/-cl8Td-xoGI.

Remark 11 In the simulation results and experimental results, time-delays are introduced to illustrate the influence of the velocity sensor faults on the control of a quadrotor. However, in practical application of the fault-tolerant control law, there is no need to introduce any time-delays. The fault-tolerant control law can be activated as soon as the fault is detected when the value of J_{det} exceeds the value of J_{th}.

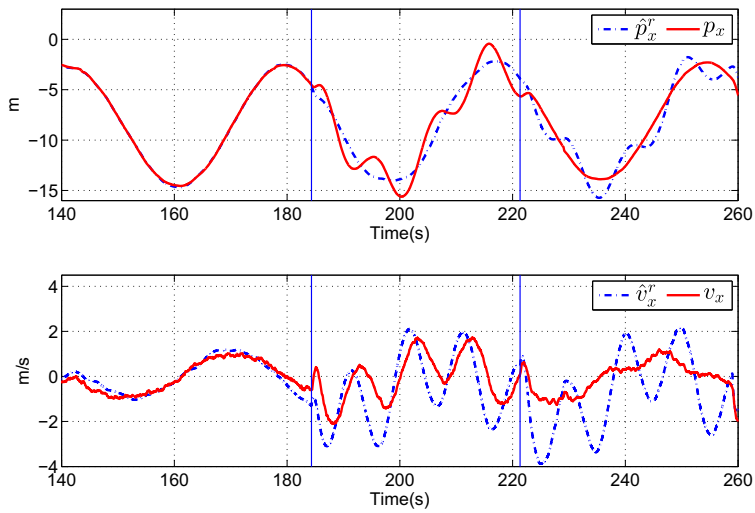

Fig. 17 State estimation in the residual generator in case 2 of the experiment

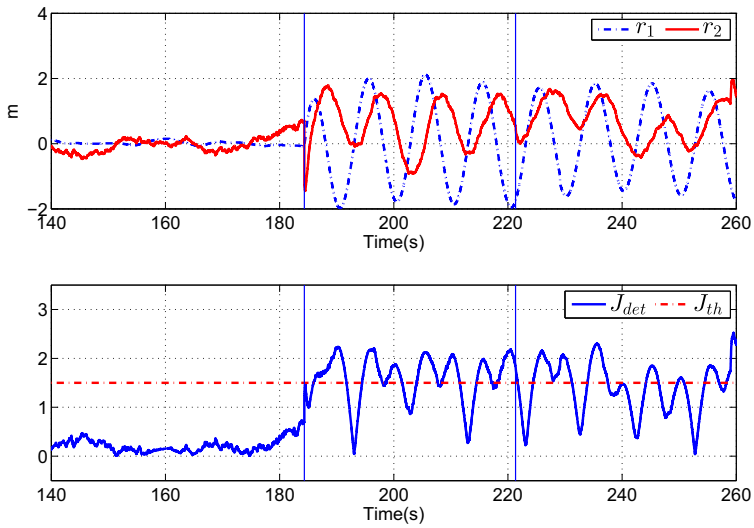

Fig. 18 Residuals and the residual evaluation function in case 2 of the experiment

Remark 12 In the simulation, since a second-order integrator is used to develop the model of the quadrotor, the fault estimation and fault-tolerant control scheme in the paper is valid even though the magnitude of the velocity sensor fault is very large. Different from the simulation, in practical experiments, the amplitude of the velocity sensor fault will influence the model of a quadrotor. Hence, the effective application of the fault estimation and fault-tolerant control law in the paper requires that the magnitude of the velocity sensor fault is limited.

In our experiments, when the velocity sensor fault is a constant signal, the maximum fault magnitude is $3m/s$. When the velocity sensor fault is a time-varying signal, the maximum fault magnitude has a relationship with the frequency of the fault signal. In general, the larger the frequency is, the less the maximum magnitude of the velocity sensor fault is.

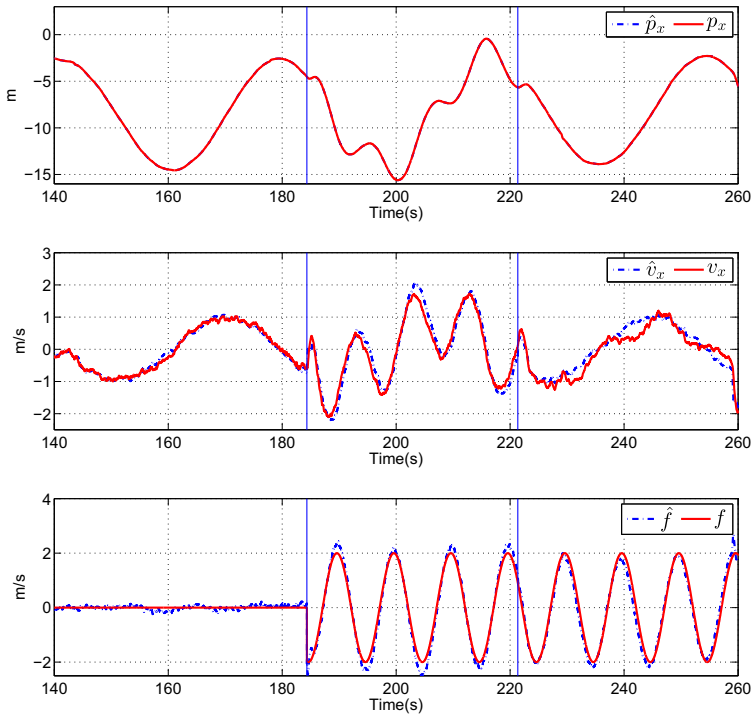

Fig. 19 States and fault estimation in the fault estimator in case 2 of the experiment

5 Conclusion

In the paper, the problems of fault diagnosis and active fault-tolerant control for a quadrotor with velocity sensor faults have been addressed. In free fault cases, a two-level controller composed of a PD controller and a PID controller have been developed to warrant that the quadrotor is able to track the given trajectory. Fault detection has been achieved by using an observer-based residual generator, and fault estimation has been achieved by utilizing an augment variable observer. The uniformly ultimately bounded property of the augment variable observer has also been proved by means of LMIs. By combining the external-loop PD controller and the fault estimation results, the fault-tolerant control law has been proposed. The effectiveness of the scheme has been illustrated by simulations and experiments.

Acknowledgments This work was supported by National Natural Science Foundation of China (NSFC) under Grants 61490701, 61210012, 61290324, Tsinghua University Initiative Scientific Research Program and Resaerch Fund for the Taishan Scholar Project of Shandong Province of China. The work of Xiao He was also supported by the NSFC under Grants 61473163 and 61522309.

References

1. Al Younes, Y., Noura, H., Rabhi, A., EL Hajjaji, A., Al Hussien, N.: Sensor fault detection and isolation in the quadrotor vehicle using nonlinear identity observer approach. In: 2013 Conference on Control and Fault-Tolerant Systems (SysTol), pp. 486–491. IEEE (2013)
2. Berbra, C., Lesecq, S., Martinez, J.: A multi-observer switching strategy for fault-tolerant control of a quadrotor helicopter. In: 2008 16th Mediterranean Conference on Control and Automation, pp. 1094–1099. IEEE (2008)
3. Bouadi, H., Aoudjif, A., Guenifi, M.: Adaptive flight control for quadrotor UAV in the presence of external disturbances. In: 2015 6th International Conference on Modeling, Simulation, and Applied Optimization (ICMSAO), pp. 1–6. IEEE (2015)
4. Bresciani, T.: Modelling, identification and control of a quadrotor helicopter. Department of Automatic Control Lund University (2008)
5. Cen, Z., Noura, H., Susilo, T.B., Al Younes, Y.: Robust fault diagnosis for quadrotor UAVs using adaptive Thau observer. J. Intell. Robot. Syst. **73**(1-4), 573–588 (2014)
6. De Lellis, M., De Oliveira, C.: Modeling, identification and control of a quadrotor aircraft. Czech Technical University, Praga (2011)
7. Freddi, A., Longhi, S., Monteriu, A.: A model-based fault diagnosis system for a mini-quadrotor. In: Proceedings 2009 7th Workshop on Advanced Control and Diagnosis, pp. 19–20 (2009)
8. Gong, M., Li, X., Zhou, J.: Robust tracking control for robot based on backstepping method. J. Shandong Univ. Sci. Technol.(Nat. Sci.) **25**(3), 32–35 (2006)
9. Li, J., Li, Y.: Dynamic analysis and PID control for a quadrotor. In: 2011 International Conference on Mechatronics and Automation (ICMA), pp. 573–578. IEEE (2011)
10. Lopez-Estrada, F.R., Ponsart, J.C., Theilliol, D., Astorga-Zaragoza, C., Zhang, Y.: Robust sensor fault diagnosis and tracking controller for a UAV modelled as LPV system. In: 2014 International Conference on Unmanned Aircraft Systems (ICUAS), pp. 1311–1316. IEEE (2014)
11. Madani, T., Benallegue, A.: Backstepping control for a quadrotor helicopter. In: 2006 IEEE/RSJ International Conference on Intelligent Robots and Systems, pp. 3255–3260. IEEE (2006)
12. Nguyen, H., Berbra, C., Lesecq, S., Gentil, S., Barraud, A., Godin, C.: Diagnosis of an inertial measurement unit based on set membership estimation. In: 2009. MED'09. 17th Mediterranean Conference on Control and Automation, pp. 211–216. IEEE (2009)
13. Qin, L., He, X., Zhou, D.: Fault-tolerant cooperative output regulation for multi-vehicle systems with sensor faults. International Journal of Control (2016). doi:10.1080/00207179.2016.1242026
14. Qin, L., He, X., Zhou, Y., Zhou, D.: Fault-tolerant control for a quadrotor unmanned helicopter subject to sensor faults. In: 2016 International Conference on Unmanned Aircraft Systems (ICUAS), pp. 1280–1286. IEEE (2016)
15. Rafaralahy, H., Richard, E., Boutayeb, M., Zasadzinski, M.: Simultaneous observer based sensor diagnosis and speed estimation of unmanned aerial vehicle. In: 2008. CDC 2008. 47th IEEE Conference on Decision and Control, pp. 2938–2943. IEEE (2008)
16. Ranjbaran, M., Khorasani, K.: Fault recovery of an under-actuated quadrotor aerial vehicle. In: 2010 49th IEEE Conference on Decision and Control (CDC), pp. 4385–4392. IEEE (2010)
17. Rich, M.: Model development, system identification, and control of a quadrotor helicopter. Ph.D. thesis. Iowa State University (2012)
18. Saberi, A., Salmasi, F.R., Najafabadi, T.A.: Sensor fault-tolerant control of wind turbine systems. In: 20145th Conference on Thermal Power Plants (CTPP), pp. 40–45. IEEE (2014)
19. Sadeghzadeh, I., Zhang, Y.: A review on fault-tolerant control for unmanned aerial vehicles (UAVs). Infotech @ Aerospace, St. Louis, MO (2011)
20. Santos, M., López, V., Morata, F.: Intelligent fuzzy controller of a quadrotor. In: 2010 International Conference on Intelligent Systems and Knowledge Engineering (ISKE), pp. 141–146. IEEE (2010)
21. Shames, I., Teixeira, A.M., Sandberg, H., Johansson, K.H.: Distributed fault detection for interconnected second-order systems. Automatica **47**(12), 2757–2764 (2011)

22. Shi, J., He, X., Wang, Z., Zhou, D.: Distributed fault detection for a class of second-order multi-agent systems: an optimal robust observer approach. IET Control Theory Appl. **8**(12), 1032–1044 (2014)
23. Tan, C.P., Edwards, C.: Sliding mode observers for robust detection and reconstruction of actuator and sensor faults. Int. J. Robust Nonlinear Control **13**(5), 443–463 (2003)
24. Wang, C., Sun, X.: Research and design of an adaptive global sliding mode variable structure controller. J. Shandong Univ. Sci. Technol.(Nat. Sci) **28**(1), 64–69 (2009)
25. Zhang, K., Jiang, B., Cocquempot, V., et al.: Adaptive observer-based fast fault estimation. Int. J. Control Autom. Syst. **6**(3), 320 (2008)
26. Zhang, Y., Chamseddine, A.: Fault tolerant flight control techniques with application to a quadrotor UAV testbed INTECH Open Access Publisher (2012)
27. Zhang, Y., Chamseddine, A., Rabbath, C., Gordon, B., Su, C.Y., Rakheja, S., Fulford, C., Apkarian, J., Gosselin, P.: Development of advanced FDD and FTC techniques with application to an unmanned quadrotor helicopter testbed. J. Franklin Inst. **350**(9), 2396–2422 (2013)

Liguo Qin received the B.E. degree in automation in 2011 from Shangdong University, Shandong, China. He is now a Ph.D. candidate in the Department of Automation, Tsinghua University, Beijing, China. His research interests include distributed fault diagnosis, fault-tolerant control for multi-agent systems and fault diagnosis for unmanned helicopters.

Xiao He received the B.E. degree in information technology from the Beijing Institute of Technology, Beijing, China, in 2004, and the Ph.D. degree in control science and engineering from Tsinghua University, Beijing, in 2010.

Currently, he is a a tenure track Associate Professor with the Department of Automation, Tsinghua University. He has authored more than 30 papers in refereed international journals. His research interests include networked filter and control, and networked fault diagnosis and isolation and their application.

Dr. He is now a Full Member of Sigma Xi, the Scientific Research Society, a Senior Member of Chinese Association of Automation (CAA). He is an Associate Editor of the JOURNAL OF THE FRANKLIN INSTITUTE.

Rui Yan received the B.S. degree in automatic control from Beihang University, Beijing, China in 2015. He is currently a Ph.D. candidate in Department of Automation, Tsinghua University, Beijing, China. His research interests include differential games, cooperative control of multi-agent systems, and formation control.

Donghua Zhou received the B.Eng., M.Sci., and Ph.D. degrees in electrical engineering from Shanghai Jiaotong University, Shanghai, China, in 1985, 1988, and 1990, respectively.

He joined Tsinghua University, Beijing, China, in 1997, and was a Professor and the Head of the Department of Automation, from 2008 to 2015. He is now the Vice President of the Shandong University of Science and Technology, Qingdao, China. He has authored and coauthored over 130 peer-reviewed international journal papers and 6 monographs in the areas of process identification, fault diagnosis, fault-tolerant control, reliability prediction, and predictive maintenance.

Dr. Zhou is a Member of the International Federation of Automatic Control (IFAC) Technical Committee on Fault Diagnosis and Safety of Technical Processes, and the Associate Chairman of the Chinese Association of Automation (CAA). He was also the National Organizing Committee (NOC) Chair of the 6th IFAC Symposium on SAFEPROCESS, 2006.